Relazione MoU INAF-CINECA

TITLE OF THE PROJECT:

A numerical study of a new class of astrophysical objects: the isolated star-forming gas cloud SECCO 1 (Year: 2018)

Francesco Calura - Osservatorio di Astrofisica e Scienza dello Spazio di Bologna

1 Scientific case

Within a survey aimed at looking for stellar counterparts in compact HI clouds[1], ongoing star formation was found within an isolated gas cloud lying in the Virgo cluster (Bellazzzini et al. 2018, B18). The mass budget of this stellar system, named SECCO 1, is dominated by neutral hydrogen ($M_{HI} \sim 10^7 M_{\odot}$), while the stellar mass is $M_* \sim 10^5 M_{\odot}$, with a metallicity 12+log(O/H)=8.38± 0.11, much higher than that of dwarf galaxies of similar mass. This implies that the cloud could have been stripped from a large galaxy but, in fact, SECCO 1 lies several hundreds of kpc apart from any known galaxy within the Virgo cluster.

Indeed, all the known properties of SECCO 1 lie in the range covered by star-forming gas clumps observed in the extended tails of ram pressure stripped gas in the so-called *jellyfish* galaxies (Poggianti et al. 2019 and references therein). The crucial difference with these systems is the extreme isolation of SECCO 1. This cloud could have travelled away from its parent galaxy for a long time (of the order of 1 Gyr) within the Intra Cluster Medium (ICM) of Virgo, preserving the conditions to form stars today, in spite of not being gravitationally bound (B18). Moreover, five additional candidate siblings of SECCO 1 were recently confirmed (the work is in prep., but a preliminary list was presented in Sand et al. 2017). Hence, SECCO 1 may represent the prototype of a new class of stellar systems.

Seveal important questions are raised by this finding, including the possibility that a cold gas cloud may survive in the hot ICM for a timescale of 1 Gyr and what are the roles played by key physical parameters in its evolution.

In a previous paper (B18) three-dimensional (3D) hydrodynamical simulations of an initially cold ($T \sim 5000$ K) gas cloud moving subsonically (but with a large speed, ∼200 km/s) through a very hot ($T \sim$ a few 10^6 K) medium were presented. Their results, partly carried on in a previous MoU INAF-CINECA project (PI: F. Calura, year: 2017), indicated that the cloud was able to preserve ≃75% of its initial content of cold gas during its 1 Gyr -long flight, while the remaining ≃25% was evaporated into the hot medium. The cloud also experienced a considerable morphological evolution, mostly driven by Kelvin-Helmholtz instabilities (KHI).

Important physical ingredients were missing in the simulation, including the self-gravity of the cloud.

Additional numerical experiments are needed to test further the role of the environment in determining the survivability of the cloud. In particular, how does the thermal state of the ICM affect the evolution of the cloud? What is the effect of a different relative velocity between SECCO 1 and the ICM on its long-term evolution? Last but not least, what are the effects of star formation and stellar feedback? In order to address these issues, in this project we performed new high-resolution, 3D simulations aimed at describing the most important processes determining the evolution of SECCO 1 and its interaction with the ICM. All the results presented here are in Calura et al. (2020).

2 Simulation Setup

Our setup is designed to recreate the fast motion of the cloud in the hot ICM of the Virgo cluster. The code used is a customized version of the grid-based, Adaptive Mesh Refinement (AMR) hydro-code RAMSES (Teyssier 2002). In our Cartesian Grid, the computational box has a volume of $L_{box}^3 = (40 \text{ kpc})^3$, chosen in order to largely contain the whole cloud and, as much as possible, the extent of instabilities. For a given setup, in general more simulations are run at various resolution and starting from the same initial conditions, in order to check numerical convergence. The maximum spatial resolution used in our simulations is of 76 pc.
The initial radius of the spherical gas cloud is ∼ 3.7 kpc. In our 'wind tunnel' numerical experiment, the

[1]SECCO survey, see `http://www.bo.astro.it/secco`

Table 1: Parameters defining the initial conditions of the models investigated in our simulations. First colums is model name, second column is cloud density, third column is cloud temperature, fourth column is density of the ICM, fifth column is temperature of the ICM, sixth column is the cloud velocity. Seventh and eighth columns indicate whether gravity and star formation are activated in the model, respectively.

MODEL	ρ_{cl} (g/cm^3)	T_{cl} (K)	ρ_{ICM} (g/cm^3)	T_{ICM} (K)	v_{cl} $(km/2)$	Gravity	SF
Standard	3×10^{-26}	10^4	2.5×10^{-29}	5×10^6	200	N	N
T1E7K	3×10^{-26}	10^4	2.5×10^{-29}	10^7	200	N	N
Supersonic	3×10^{-26}	10^4	2.5×10^{-29}	5×10^6	400	N	N
Gravity	3×10^{-26}	10^4	2.5×10^{-29}	5×10^6	200	Y	N
Star Formation	3×10^{-26}	10^4	2.5×10^{-29}	5×10^6	200	Y	Y

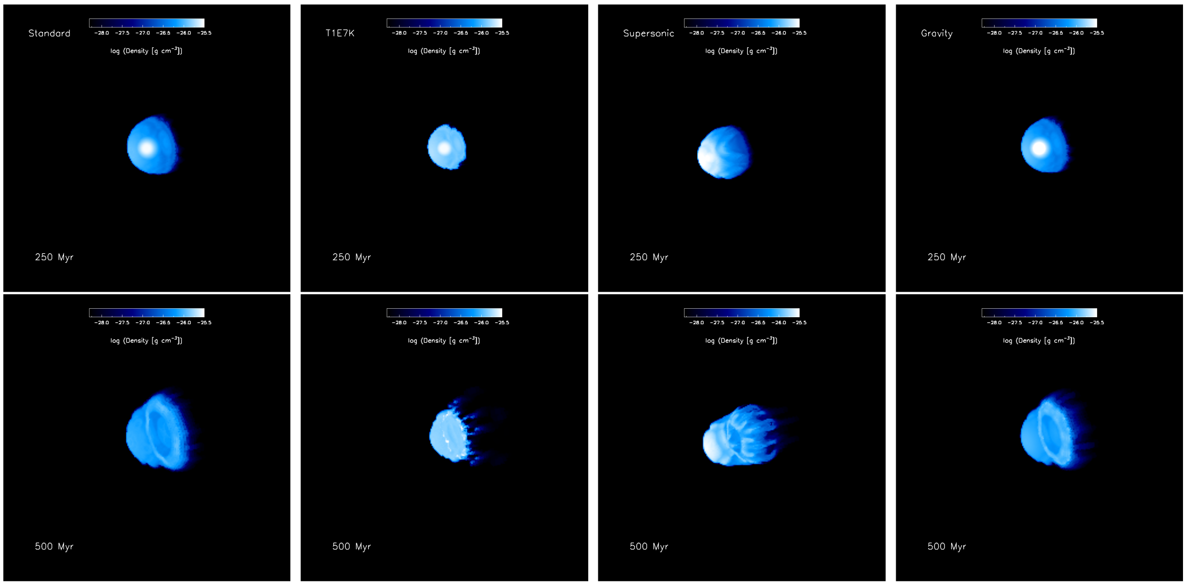

Figure 1: Three-dimensional gas density distribution in our simulations at various time steps for the Standard (first column), T1E7K (second column), Supersonic (third column) and Gravity (fourth column) simulations. In each column, upper (lower) panels describe the model at 250 Myr (500 Myr). The assumed rotation angle with respect to the x- and y- axis is of 30 degrees.

reference frame is placed at the centre of the cold gas cloud, and since the start of the simulation the hot ICM gas moves continuously along the x-axis. New fast, hot gas is continuously allowed to flow inside our computational box from one of the boundaries and again moving parallel to the x-axis, from left to right.
A description of the star formation module can be found in Calura et al. (2019). Also supernova feedback is included in this case.
The parameters describing the initial conditions of the models investigated in this paper are reported in Table 2.

3 Results

Fig. 1 shows 3D volume-rendering maps of the gas density at different times for the non-star forming simulations, where the top (bottom) panels show the gas distribution of the models computed at 250 Myr (500 Myr). In all cases, the system evolves from a from an initial spherical shape (as assumed here) to an umbrella-like or jellyfish-like shape. With respect to the standard model, a larger temperature value (10^7 K) assumed for the ICM produced, at any time, a more compressed gas cloud. The aspect of the instabilities at the edges of the cloud is different, in that they appear more elongated, spatially separated and curled with respect to the standard case. In the case of a supersonic relative velocity between the cloud and the ICM, the cloud undergoes a strong compression at its front, and its stretching occurs mostly along the direction of motion. In our hydrodynamic simulation in which the self-gravity of the gas cloud was taken into account, on large scales and on a long timescale the properties of the cloud are very similar to the ones of the standard model, which confirms that the role of gravity is marginal in its large-scale evolution.

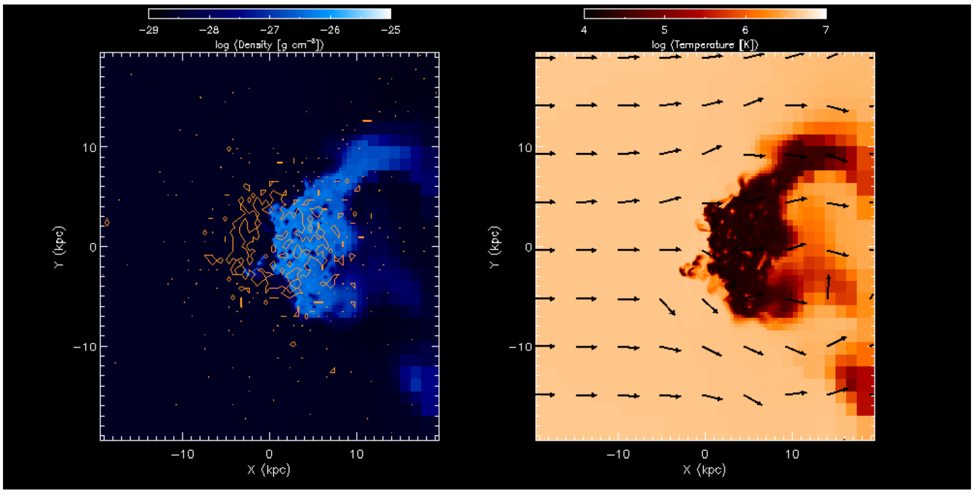

Figure 2: Two-dimensional slices in the x-y plane of the gas density (left panel) and temperature (right panel) distribution in our simulation with star formation, at 1 Gyr. The orange contours in the density maps describe the distribution of the stars, and represent regions which enclose > 50% of stellar mass. The arrows in the 2d temperature map are plotted to describe the velocity field of the gas.

However, we have found that, even if gravity does not prevent the growth of large scale instabilities, it hinders the development of small-scale instabilities, in particular on the front of the cloud.
All the models which do not include star formation show a similar evolution of the cold gas fraction with time, and similar values at 1 Gyr. Final values for the retained cold gas fraction range between 0.75 and ∼0.8, Sonsistent with the standard model.
The results of the simulation which include star formation and feedback are presented in Fig. 2, in which two-dimensional maps of the density and temperature distribution are shown in the left and right panel, respectively, computed at 1 Gyr. The orange countour in the left panel shows the stellar distribution, whereas the black arrows in the right panel describe the velocity field. The end state of the resulting (unbound) stellar system presents both differences as well as intriguing similarities with the observed structure. Throughout its entire evolution, due to inhomogeneous SN explosions, the appearence of the cloud is much more asymmetric than in the previous cases. The combined effects of the gravity of the stars and of the compression of the cloud in its centre as due to stellar feedback have a strong influence on the properties of the cloud. Due to an enhanced compression of the gas in the outskirts, stellar feedback has the global effect of facilitating the develompment of instabilities. SN feedback facilitates the heating of the cold gas. In this case, after 1 Gyr, 50% of the initial cold gas is present in the box.

4 Other Remarks

The present project was not meant as a pilot for larger projects (such as ISCRA or PRACE). The present project has already led to the production of one scientific paper, 'Hydrodynamic simulations of an ultra-diffuse star-forming cloud in the Virgo cluster' by F. Calura, M. Bellazzini and A. D'Ercole, currently submitted to the Montly Notices of the Royal Astronomical Society. A few test simulations were also run for another published work, 'Formation of second-generation stars in globular clusters' by F. Calura et al., 2019, MNRAS, 489, 3269, in which a setup upon which the one of the current simulations is based was first presented.

The advantages of having obtained the CPU time by means of the MoU CINECA-INAF agreement instead of applying to a generic call is mainly the fast, positive answer which came very soon after our application, as well as the possibility of having promptly both the CPU hours and the requested facilities ready for our use.

5 Bibliography

Bellazzini M., Armillotta, L., Perina, S., et al., 2018, MNRAS, 476, 4565 (B18)
Calura F., Bellazzini M., D'Ercole, A., 2020, MNRAS, submitted
Calura F., D'Ercole A., Vesperini E., Vanzella E., Sollima A., 2019, MNRAS, 489, 3269
Poggianti B. M., et al., 2019, ApJ, 887, 155

Sand, D.J., Seth, A.C., Crnojević, D., et al., 2017, ApJ, 843, 134
Teyssier, R., 2002, A&A, 385, 337